The Effects of Soil Gradation on System Level Dynamic Response

Alexander P. Sturm¹ and Jason T. DeJong, Ph.D.²

¹Graduate Student, Dept. of Civil and Environmental Engineering, Univ. of California at Davis, Davis, CA. E-mail: apsturm@ucdavis.edu

²Professor, Dept. of Civil and Environmental Engineering, Univ. of California at Davis, Davis, CA. E-mail: jdejong@ucdavis.edu

ABSTRACT

Recent studies have focused on how the dynamic response of a clean sand changes with increasing fines content; however, there remains a limited understanding regarding the effects of increasing coarse content. This study aims to elucidate these effects at a system level via centrifuge testing of two uniformly-graded and one well-graded soil mixture which range in mean grain diameter (D_{50}) from 0.18 to 2.58 mm and in coefficient of uniformity (C_U) from 1.53 to 7.44. Models of each soil mixture were prepared to approximately 50% relative density (D_R) and subjected to uniform cycles of sinusoidal acceleration at various Arias intensities (I_a). The high hydraulic conductivity (k) of the coarsest, uniformly-graded mixture prevented significant excess pore pressure generation; however, liquefaction was induced in the other two mixtures. Furthermore, the well-graded mixture exhibited a stronger dilative tendency than the clean sand. The centrifuge results were compared to cyclic direct simple shear (DSS) results in order to consider the complementary perspectives that centrifuge and element testing can provide.

INTRODUCTION

Standard of practice assumes that the case-history based liquefaction triggering curves, developed primarily for clean sands, will be generally applicable when large particles are present. This practice requires refinement as there is limited understanding regarding particlesize effects on liquefaction potential and dynamic response.

Numerous studies have conducted undrained, cyclic element tests on gravelly soils to evaluate their dynamic response. Early studies focused on large-scale triaxial testing of composite samples (Wong et al. 1974) and methods to minimize the effects of membrane penetration (Evans & Seed, 1987). Studies from Japan (Goto et al., 1994) focused on the dynamic response of natural deposits sampled via in situ ground freezing. A more recent study (Hubler et al., 2017) has probed the parameter space using large-scale direct simple shear equipment and composite gravelly mixtures. Overall, each study has further contributed to the knowledge base; however, ambiguity remains, and no systematic model of a gravelly soil's liquefaction potential or dynamic response has been developed in research or adopted in practice.

This paper aims to study the effects of soil gradation on system level dynamic response via centrifuge testing of composite soil mixtures. The field-scale simulation offered by centrifuge testing is expected to provide a distinct perspective which will complement the element testing available in literature. The authors caution that a size-based criterion alone may not adequately capture the full range of parameters which would influence dynamic response. Inevitably, a soil which includes large particles can exhibit a wider range of attributes (i.e. C_u , C_c , roundness, sphericity, etc.) than a clean sand. It is hypothesized that this wider range of attributes will affect relevant material properties (i.e. e_{min} , e_{max} , k, ϕ' , G, etc.) and, therefore, the dynamic response.

TESTING PROGRAM

Soil Mixtures: Four, uniformly-graded soils with mean grain diameters (D_{50}) ranging from 0.18 to 2.58 mm were combined in different proportions to create soil mixtures for testing. These base soils are of Pleistocene marginal-marine deposition and were not modified during mining; thus, their minerology, roundness and sphericity are indicative of their deposition (Nichols, 2009). Overall, these attributes are expected to affect the soils' dynamic response; thus, it was considered key to ensure that their variation was consistent with natural, depositional processes. Throughout this paper the four base soils will be referred to via a letter designation, with Soil A having the smallest D_{50} and Soil D having the largest.

Three soil mixtures were constructed from the base soils: two uniformly-graded (100A, 100D) and one well-graded (25ABCD). The mixtures are named based on the percent by mass of the base soils they contain. For example, the well-graded mixture (25ABCD) contains 25% by mass of base soils A, B, C and D. Figure 1 shows the grain size distribution curves and photos of the three soil mixtures. The index properties of each soil mixture were characterized using standardized methods (Shepard, 2018) and are summarized in Table 1.

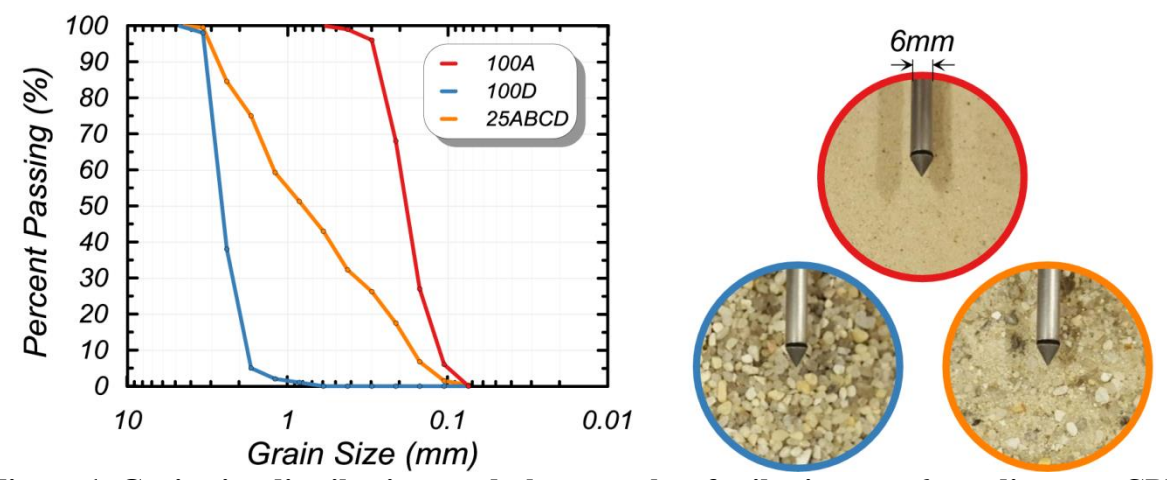


Figure 1. Grain size distributions and photographs of soil mixtures. 6mm diameter CPT shown for scale.

T 11 1		4 •	e •1	• 4
Ighia i	A varaga indav	nranartias	At CAIL	mivfiirac
I abit 1. I	Average index	DI ODCI UCS	OI SOH	minatur Co.

Soil	D ₅₀ (mm)	C_{u}	C_c	Roundness	Sphericity	G _s	e_{min}	e_{max}	k (cm/sec)	USCS
100A	0.18	1.68	1.02	0.69	0.79	2.62	0.58	0.88	0.017	SP
100D	2.58	1.53	1.00	0.51	0.74	2.60	0.54	0.81	2.271	SP
25ABCD	0.80	7.44	0.67	0.62	0.77	2.61	0.30	0.54	0.021	SW

Centrifuge Testing: Three models were constructed, one from each soil mixture, and tested on the 1 m radius centrifuge at the UC Davis Center for Geotechnical Modeling. Each model was prepared to an initial relative density (D_R) of approximately 50% via dry pluviation into a flexible shear beam container. Specialized pluviation procedures were developed for each soil mixture to meet the target density and prevent segregation (Shepard, 2018). All testing was conducted at a centrifugal acceleration of 80 g in order to simulate a 9.8 m thick deposit. A curved soil surface was used to model level-ground conditions under the radial g-field imposed by the centrifuge (Figure 2).

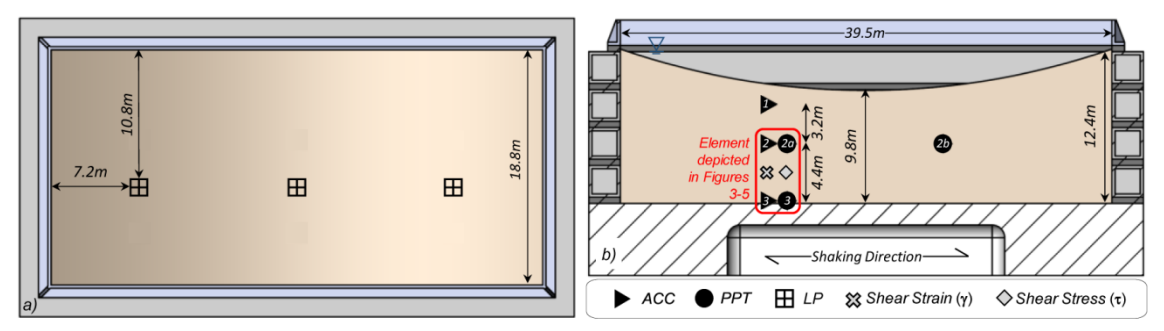


Figure 2. Centrifuge model layout in prototype units. a) Plan view. b) Cross section view.

The models were saturated via a top-down procedure with a fluid 40 times the viscosity of water to minimize the scaling conflict between dynamic and diffusion time (Garnier et al., 2007) while maintain a practically-realizable model construction sequence. The incongruity between glevel and fluid viscosity is expected to influence the rate of pore pressure generation and dissipation; however, the effect is expected to be constant across all models.

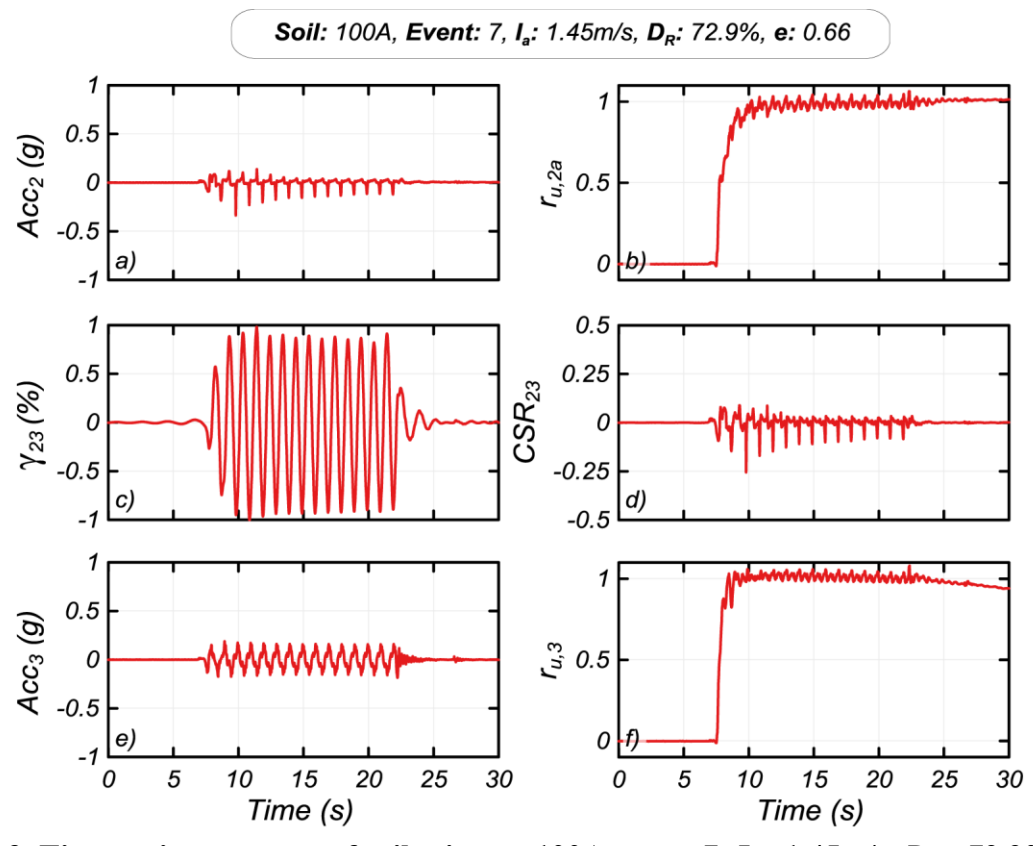


Figure 3. Time series response of soil mixture 100A, event 7. I_a = 1.45m/s, D_R = 72.9%, e = 0.66.

Each model was subjected to multiple dynamic loading events of progressively increasing Arias Intensity (I_a). Fifteen, uniform cycles of a 1 Hz, sinusoidal acceleration were applied to the models during each loading event. The acceleration was input at the base of the model and propagated upward through the soil column. The soil response was measured via accelerometers (ACC), pore pressure transducers (PPT) and linear potentiometers (LP) at the locations shown in

Figure 2. The measured acceleration time histories were used to compute shear stress (τ) and shear strain (γ) via the procedures outlined in Kamai & Boulanger (2010) and Brandenberg et al. (2010), respectively.

The models progressively densified in response to dynamic loading. The evolution of relative density was monitored via surface settlement measurements from both the linear potentiometers and a high-accuracy Vernier scale. On average, it took 30 loading events for the soils to densify from 50 to 95%. Additional details regarding the loading sequence, dynamic measurements and analysis procedures are provided in Sturm et al. (2018).

Direct Simple Shear Testing: Cyclic, direct simple shear (DSS) testing was performed on each soil mixture under saturated, constant volume conditions. Changes in vertical effective stress were equated to changes in pore water pressure that would have occurred during undrained loading. This is commonly referred to as equivalent undrained testing. Each specimen was prepared, via dry pluviation, to a relative density of approximately 50% and consolidated under a vertical effective stress of 100 kPa. Multiple tests were conducted at various cyclic stress ratios (CSR = τ/σ'_{Vo}).

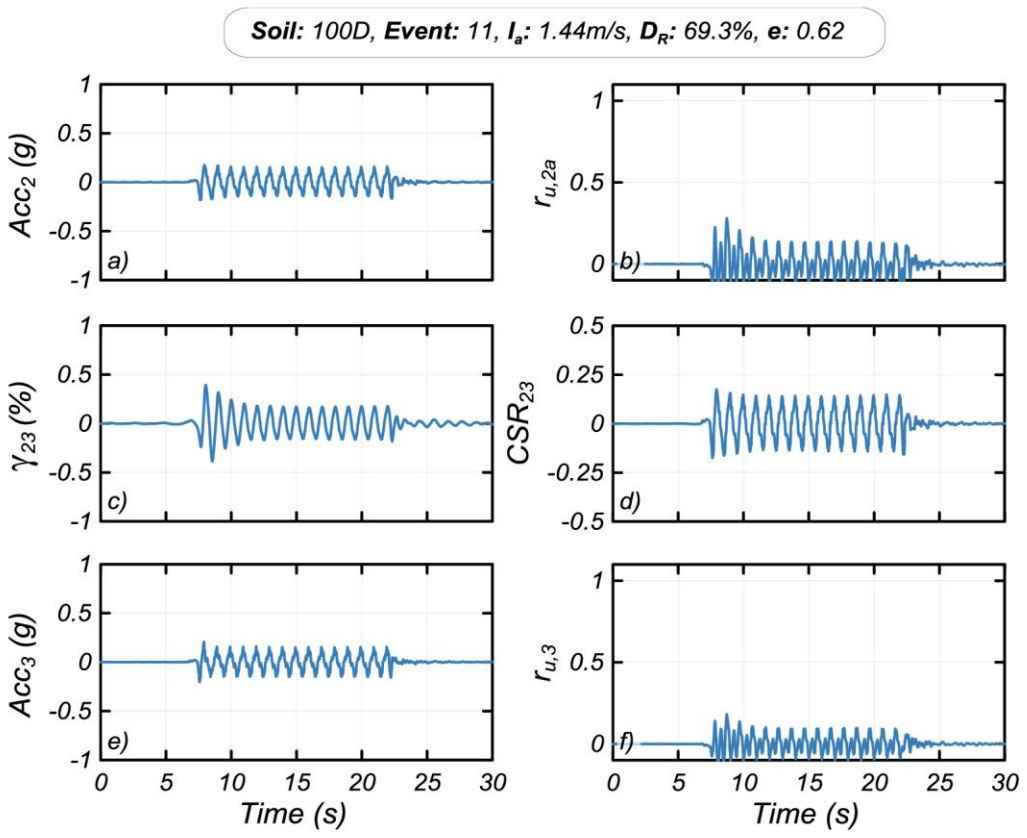


Figure 4. Time series response of soil mixture 100D, event 11. $I_a = 1.44$ m/s, $D_R = 69.3\%$. e = 0.62.

RESULTS

Centrifuge Testing: The authors aim to isolate the influence of gradation by comparing the soil mixtures' response at points of similar capacity (D_R) and demand (I_a). Loading events 7, 11 and 10 will be analyzed for soil mixtures 100A, 100D and 25ABCD, respectively. These events represent a point of similar capacity was at a relative density between 69 and 73%

and was subjected to a 1.44 to 1.47 m/s Arias Intensity loading event.

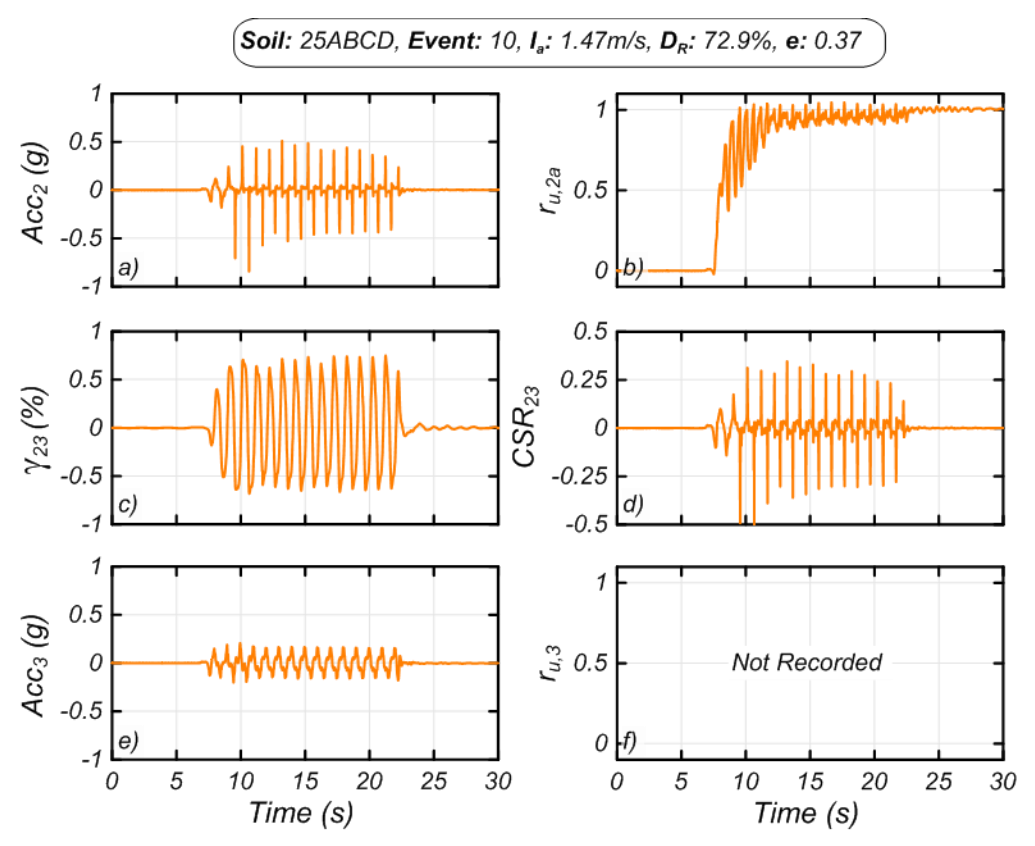


Figure 5. Time series response of soil mixture 25ABCD, event 10. I_a = 1.47m/s, D_R = 72.9%. e = 0.37.

Figures 3-5 show the soils' response at the point of similitude for an element extending from mid-depth down to the base of the model (highlighted in red in Figure 2). Measured time histories of acceleration and excess pore pressure ratio (r_u) are presented at mid-depth (subplots a-b) and the base of the model (subplots e-f). The calculated time histories of shear strain (γ) and CSR are presented in subplots c and d.

Figure 3 presents time histories of dynamic response for soil mixtures 100A during loading event 7. Pore pressure builds rapidly, initiating liquefaction (i.e. $r_u > 0.95$) in approximately 1.5 cycles at both mid-depth and the base of the model (Figures 3b, 3f). Following initial liquefaction, the soil column softens and can no longer effectively transmit shear stresses, hence the acceleration at mid-depth is consistently lower than the acceleration at the base of the model (Figures 3a, 3e). This softening of the soil column is responsible for the reduction in CSR following initial liquefaction (Figure 3d). Single amplitude shear strains reach approximately 1% during every post-liquefaction cycle. Prior to liquefaction, shear strain reaches a maximum of 0.52% (Figure 3c). Just before load reversal, the soil dilates, pore pressure momentarily decreases and the soil stiffens. This stiffening limits the development of shear strains while simultaneously causing a sharp increase in CSR.

Figure 4 presents time histories of dynamic response for soil mixtures 100D during loading event 11. Liquefaction is not initiated at any point during the loading event. While excess pore pressure responds to the input acceleration it never exceeds 0.3 at both mid-depth and the base of the model (Figure 4b, 4f). Barring liquefaction, the soil column does not soften substantially;

thus, the acceleration measured at mid-depth is nearly identical to the acceleration input at the base of the model (Figure 4a, 4e). This results in a uniform CSR time series with peaks of approximately 0.15 and relatively uniform shear strain time series with average, single amplitude maximums of 0.2 (Figure 4c, 4d). The soil skeleton does contract and dilate as evidenced by the pore pressure response, but effective stress remains sufficiently high that the soil column behaves as a rigid body.

Figure 5 presents time histories of dynamic response for soil mixtures 25ABCD during loading event 10. The excess pore pressure ratio at mid-depth first exceeds 0.95 after 1.5 cycles. Prior to this point of initial liquefaction and for approximately 3 cycles after, the pore pressure ratio rapidly reduced as the soil dilates prior to stress reversal. After approximately 5 cycles the excess pore pressure ratio adopts a stable, repeating pattern. This response cannot be corroborated at the base of the model due to a damaged sensor (Figures 5b, 5f). Prior to initial liquefaction, the acceleration measured at mid-depth is nearly identical to the acceleration input at the base of the model. Following initial liquefaction, the acceleration at mid-depth is amplified via a series of dilation spikes prior to stress reversals (Figures 5a, 5e). These dilation spikes are mirrored in the time history of CSR (Figure 5d). Single amplitude shear strains reach approximately 0.7% during every cycle and appear to be independent of pore pressure and/or stress (Figure 5c).

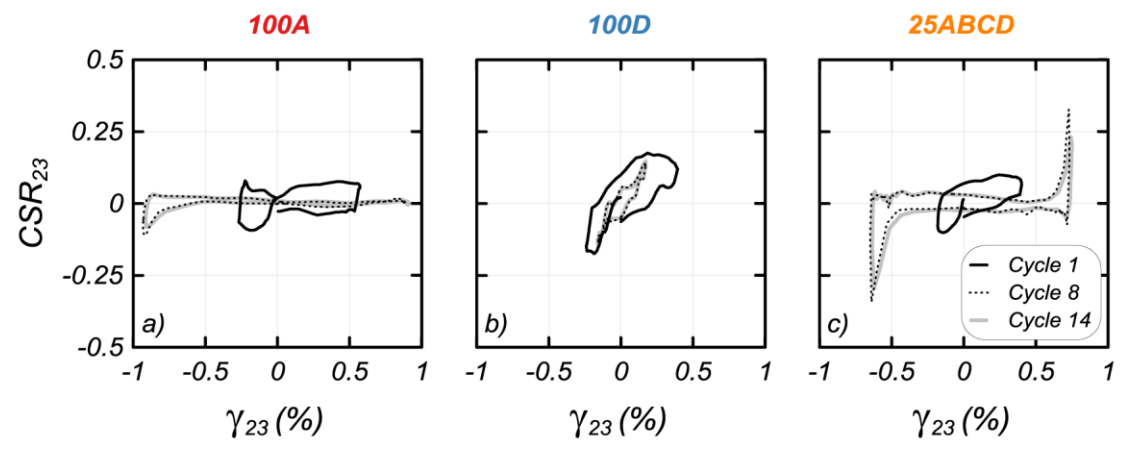


Figure 6. Stress-strain response for cycles 1, 8 and 14 for soil mixtures a) 100A, event 7, b) 100D, event 11 and c) 25ABCD, event 10.

Figure 6 presents the relationship between CSR and shear strain at the point of similitude for soil mixtures 100A, 100D and 25ABCD. Cycles 1, 8 and 14 are shown to elucidate the evolution of dynamic response throughout a single loading event. Cycle 1 precedes initial liquefaction for all three soil mixtures; thus, each soil exhibits a relatively high shear stiffness which limits shear strains despite high values of CSR. Cycle 8 occurs post-liquefaction for soil mixtures 100A and 25ABCD. During this cycle, soil 100A has a low shear stiffness from ±0.8% shear strain. Evidence of dilation is observed near -0.9% shear strain as CSR begins to increase before stress reversal. In contrast, soil mixture 25ABCD begins to dilate much earlier, at approximately ±0.5% shear strain, which limits the maximum shear strains to approximately 0.7%. Soil 100D exhibits a similar response during cycles 1 and 8: stiffness and maximum CSR are approximately the same. The slight decrease in shear strains are likely a result of soil densification. The stress-strain response of cycle 14 is nearly identical to cycle 8 for all three soil mixtures. Maximum shear strains remain constant even after 5 additional loading cycles. This result is not dependent

on excess pore pressure ratio as the same behavior is observed in 100D.

Direct Simple Shear Testing: To provide context for the centrifuge results, Figure 7 presents data from a cyclic DSS test on soil 100A at a relative density of 48.5% loaded to a constant CSR of 0.08. Subplot a depicts the measured stress-strain response for cycles 1, 8 and 14 while subplots b-c present shear strain, CSR and excess pore pressure ratio verse cycle number. The pore pressure builds gradually, initiating liquefaction after 6 cycles. Following initial liquefaction, the soil column softens resulting in increased shear strains. As loading continues the soil begins to dilate, pore pressures temporarily decrease and the shear stiffness increases. This process limits strains as the CSR reaches its peak value. Upon stress reversal, the soils contracts, pore pressure builds and shear strains grow in the opposite direction. Following initial liquefaction, the shear strains continues to grow with each additional loading cycle in a process known as cyclic mobility (Idriss & Boulanger 2008). This can be seen by comparing the CSR vs shear strain loops of cycles 8 and 14 (Figure 7a).

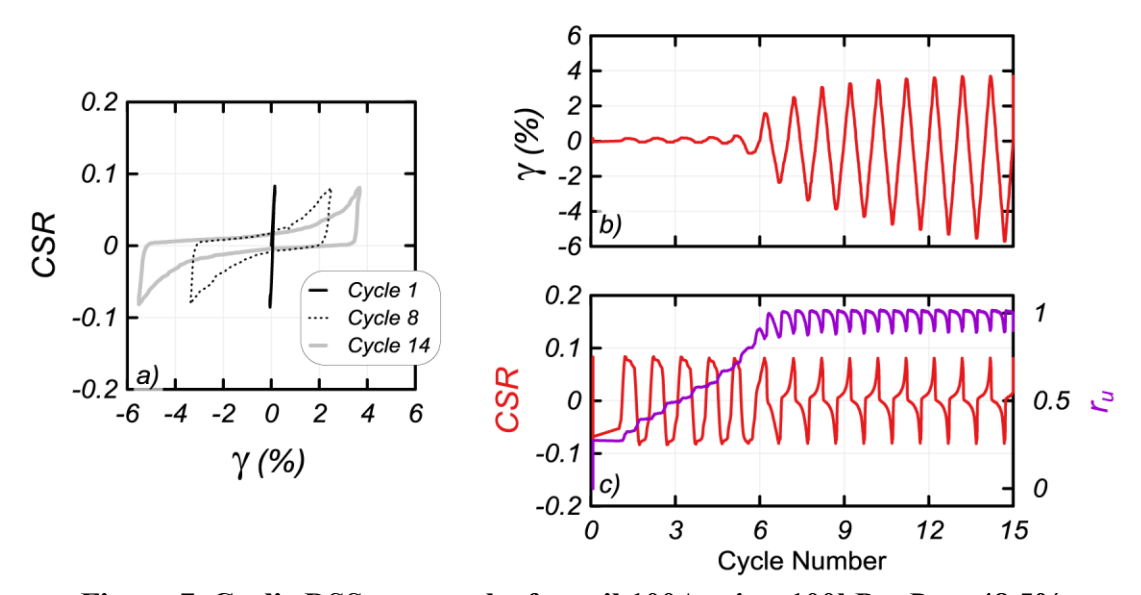


Figure 7. Cyclic DSS test results for soil 100A. σ'_{vo} = 100kPa, D_R = 48.5%.

DISCUSSION

Figures 3-5 reveal that soil mixtures 100A and 25ABCD liquefied (i.e. $r_u > 0.95$) while soil 100D did not. Liquefaction cannot occur if pore pressures dissipate faster than they are generated. The rate of pore pressure response is controlled by the soil's hydraulic conductivity (k), viscosity of the saturation fluid, rate of loading and physical boundaries. Differences in pore pressure response are attributed to differences in hydraulic conductivity since the other controlling variables were held constant. It is hypothesized that mixture 100D did not liquefy because its hydraulic conductivity is two orders of magnitude larger than the other soil mixtures (Table 1). The similarities in pore pressure response between soil 100A and 25ABCD are attributed to their similar hydraulic conductivities. Despite the presence of larger particles in mixture 25ABCD its hydraulic conductivity was nearly identical to 100A, indicating that smaller grain sizes are a controlling factor (Hazen, 1911). These system level responses cannot be observed in element testing (Figure 7c) where the undrained condition is mechanically controlled through enforcement of a constant volume condition.

Although both experienced liquefaction, soil mixture 25ABCD exhibited dilation at lower

shear strains than soil 100A (Figures 6a, 6c). As a result, soil 25ABCD sustained less maximum shear strain that soil 100A. It is hypothesized that the increased dilation of mixture 25ABCD is a result of its greater packing efficiency. The minimum and maximum void ratios of 25ABCD are systematically lower than 100A (Table 1). At the point of similitude, soil mixture 100A and 25ABCD had void ratios of 0.66 and 0.37, respectively, despite similar relative densities. The lower void ratio of mixture 25ABCD likely makes it more resistant to particle rearrangement.

During DSS testing shear strains grow with additional loading cycles (Figure 7a) whereas they remain constant during centrifuge testing (Figure 6). This may occur for two reasons. First, DSS testing imposes a constant, maximum CSR whereas the CSR imposed during centrifuge testing is a function of soil stiffness and pore pressure response. After initial liquefaction the CSR often decreases with continued shaking during centrifuge testing, which limits shear strain accumulation. Second, despite using a flexible shear beam container, the strains imposed during centrifuge testing are influenced by the boundary conditions imposed by the relative stiffness of the model container.

Rapidity of loading and constantly changing shear wave velocity (Kutter & Wilson, 1999) inherent to centrifuge testing make it difficult to accurately analyze time-dependent responses. For example, pore pressure increases upon stress reversal are clearly correlated in time under the controlled environment of DSS testing (Figure 7). While the same responses are seen in the centrifuge results, the pore pressure response often lags the load reversal for soils which experienced liquefaction (100A, 25ABCD). This phenomenon was not observed for non-liquefied soil 100D where the shear wave velocity remained high and responses were appropriately correlated in time.

CONCLUSIONS

The results of a series of centrifuge tests on coarse-grained soil mixtures has led to the following observations and conclusions:

- During centrifuge testing a soil's liquefaction potential is dependent on its hydraulic conductivity which will be governed by the smaller grain sizes (all else being equal) (Hazen, 1911). This should be considered when evaluating the liquefaction potential of coarse-grained soil deposits in the field. The presence of large particles should not reduce the liquefaction potential of a deposit unless the particles are abundant enough to increase hydraulic conductivity.
- The well-graded mixture (25ABCD) exhibited dilation at lower shear strains than the clean sand (100A). It is hypothesized that the differences in packing efficiency are responsible for the stronger dilative tendency of the well-graded mixture. Extending these findings to the field-case implies that a well-graded soil may sustain smaller deformations than a uniformly graded soil (all else being equal).
- Centrifuge testing provided insights into the system level effects of soil gradation on dynamic response. The field-scale simulation better illustrated the interplay between pore pressure response, soil stiffness, imposed CSR and generation of shear strains than element testing. While the observations offered by this system level approach are useful, they are difficult to generalize because the results are only valid for the set of conditions simulated during testing. Centrifuge testing may prove a useful tool for verification of analysis procedures (calibrated from element tests) which include the effects of soil gradation on dynamic response.

Overall, these findings emphasize the importance of recognizing the full parameter space

when considering a soil's dynamic response. Variations in a soil's attributes (i.e. C_u , C_c , roundness, sphericity, etc.) were shown to affect its material properties (i.e. e_{min} , e_{max} , k, G, etc.) and ultimately its dynamic response.

ACKNOWLEDGEMENTS

This work would not have been possible without the support from the technical staff at the UC Davis CGM: Chad Justice, Anatoliy Ganchenko, Tom Kohnke and Dan Wilson. It was a pleasure to conduct these tests with both Brian Sawyer and Greg Shepard. The training and advice provided by graduate students Mohammad Khosravi, Trevor Carey and Kate Darby is greatly appreciated. Undergraduate interns Diana Melendez, Evan Barnell, Brian Morales and Joel Given are thanked for their assistance. This work was funded by the National Science Foundation (#CMMI-1300518) and the California Department of Water Resources, Division of Safety of Dams. Any opinions, findings and conclusions or recommendations expressed in this material are those of the authors and do not necessarily reflect those of the NSF.

REFERENCES

- Brandenberg, S. J., Wilson, D. W., and Rashid, M. M. (2010). "Weighted residual numerical differentiation algorithm applied to experimental bending moment data." *J. Geotechn. Geoenviron. Eng.*, 136, 854–863.
- Evans, M.D., Seed, H. B. (1987). "Undrained cyclic triaxial testing of gravels the effect of membrane compliance." University of California, Berkeley, UCB/EERC-8.
- Garnier, J., Gaudin, C., Springman, S. M., Culligan, P. J., Goodings, D., Konig, D., Kutter, B., Phillips, R., Randolph, M. F., and Thorel, L. (2015). "Catalogue of scaling laws and similitude questions in geotechnical centrifuge modelling." *International Journal of Physical Modelling in Geotechnics*, 7(3), 01–23.
- Goto, S., Nishio, S., Yoshimi, Y. (1994). "Dynamic properties of gravels samples by ground freezing." *ASCE Ground Failures under Seismic Conditions*, (44), 141–157.
- Hazen, A. (1911). "Discusson: Dams on Sand Foundations." Transactions, ASCE, 73(11).
- Hubler, J. F., Athanasopoulos-Zekkos, A., and Zekkos, D. (2017). "Monotonic, Cyclic, and Postcyclic Simple Shear Response of Three Uniform Gravels in Constant Volume Conditions." *Journal of Geotechnical and Geoenvironmental Engineering*, 143(9), 04017043.
- Idriss, I. M., and Boulanger, R. W. (2008). *Soil liquefaction during earthquakes*. EERI, Oakland. Kamai, R., and Boulanger, R. (2011). "Characterizing localization processes during liquefaction using inverse analyses of instrumentation arrays." *Meso-Scale Shear Physics in Earthquake and Landslide Mechanics*, 219–238.
- Kutter, Bruce, Wilson, D. (1999). "De-Liquefaction Shock Waves." 7th US-Japan Workshop on Earthquake Resistant Design of Lifeline Facilities and Countermeasures Against Soil Liquefaction, MCEER-99, 295–310.
- Nichols, G. (2009). Sedimentology and stratigraphy. John Wiley & Sons.
- Shepard, G. M. (2018). "Characterization of Coarse-Grained Soil Mixes for Investigation of Penetrometer to Particle Size Effects Using Centrifuge Modeling." University of California, Davis.
- Sturm, A.P., Shepard G.M., DeJong, J.T., Wilson, D. W. (2018). "A Centrifuge Study on the Effects of Soil Gradation on Liquefaction Potential and Dynamic Response." *Dam Safety 2018*, ASDSO, Seattle, WA.

Wong, R., Seed, H.B., Chan, C. K. (1974). "Liquefaction of Gravelly Soils Under Cyclic Loading Conditions." University of California, Berkeley, EECR 74-11.